Journal of Physiology and Biochemistry
https://doi.org/10.1007/s13105-021-00851-8

ORIGINAL ARTICLE

NNMT is induced dynamically during beige adipogenesis in adipose tissues depot-specific manner

Ru Jia[1,2] · Xiaojing Wei[3] · Jianan Jiang[3] · Zhao Yang[3] · Jiaqi Huang[3] · Jing Liu[3] · Jianqun Yan[3] · Xiao Luo[3]

Received: 4 December 2020 / Accepted: 3 October 2021

Abstract

Nicotinamide N-methyltransferase (NNMT) is a novel regulator, shown recently to regulate adipose tissue energy expenditure partly through changing NAD + content, which is essential for mitochondrial. We determine whether NNMT plays important role in energy metabolism during the beige adipogenesis in vivo and in vitro. Male C57BL/6 mice at 8 weeks old were exposed to 4 °C for 1, 2, 3, 4, and 5 days, respectively. Interscapular brown adipose tissue (iBAT), inguinal subcutaneous WAT (sWAT), and epididymal WAT (eWAT) were harvested for gene and protein expression analysis and the correlation analysis. In addition, cultured primary mice brown adipocyte (BA) and white adipocyte (WA) treated with or without β3-adrenoceptor agonist (CL316, 243) were also harvested for these analyses. A combination of NNMT and its related genetic (*Nmnat1*, *Nampt*, *Cyp2e1*, *Nrk1*, *Cd38*) and proteic analyses and also the NAD + levels demonstrated the dynamical and depot-specific remodeling of NAD metabolism in different adipose tissues in response to cold exposure. While upon CL316, 243 treatment, gene expression of *Nnmt*, *Nampt*, *Cyp2e1*, and *Nrk1* was all significantly decreased in WA but not in BA. The increased NAD + amount in BA and WA during the beige adipogenesis was observed. Besides, it is demonstrated that the expression of NNMT both in sWAT and WA showed significant negative correlation with browning markers UCP-1 and PGC-1α at protein levels. Above all, NNMT was induced in WAT during the 'cold remodeling' phase and correlated negatively with the process of browning in sWAT and WA, indicating the specific role of NNMT in the regulation of energy homeostasis during the process of beige adipogenesis.

Keywords NNMT · NAD + metabolism · Beige cells · Adipose tissue · Obesity

Introduction

Adipose tissue is one of the most flexible organs in our whole body, and it has the ability to regulate the balance of energy metabolism as the environment changes. According to the morphology and function, adipose tissue can be divided into white adipose tissue (WAT) and brown adipose tissue (BAT), respectively [10]. Brown adipocytes contain numerous multicellular lipid droplets and are rich in mitochondria, which is specialized to generate heat through energy dissipation rather than shivering, while white adipocytes, on the other hand, have a single locular lipid droplet and relatively few mitochondria, which are considered to maintain energy balance throughout the body through lipid processing. More importantly, recent research has identified an intermediate type of adipocyte that is present in WAT in mammals. These cells, known as beige cells, have high expression of uncoupling protein-1 (UCP-1) and large numbers of mitochondria and exhibit multilocular lipid droplets like BAT morphology [21, 36]. The browning of adipose tissues promotes the heat production and energy consumption and keep the energy metabolism balance [4]. Therefore, perhaps not surprisingly, the activity of adipose tissue mitochondria appears to be particularly important for maintaining overall energy metabolic health during the process of beige adipogenesis.

Ru Jia and Xiaojing We contributed eqaully to this work.

✉ Xiao Luo
xluo@mail.xjtu.edu.cn

[1] Key laboratory of Shaanxi Province for Craniofacial Precision Medicine Research, College of Stomatology, Xi'an Jiaotong University, Xi'an, China

[2] Department of Prosthodontics, College of Stomatology, Xi'an Jiaotong University, Xi'an, China

[3] Department of Physiology and Pathophysiology, School of Basic Medical Sciences, Xi'an Jiaotong University Health Science Center, 76 Yanta Western Road, Xi'an, Shaanxi 710061, People's Republic of China

Published online: 26 October 2021

Mitochondria are very important organelles for the physiology of adipose tissue in many fundamental ways. As mentioned above, white adipocytes can be induced to become beige adipocytes under some certain circumstances or drugs. During this process, the number of mitochondria in the beige adipocytes increases significantly in order to perform their thermogenic functions. Recently, researchers have found that nicotinamide adenine dinucleotide (NAD) + /NADH redox coupling largely determines the mitochondrial metabolism homeostasis. And the disorders of NAD + homeostasis and mitochondrial metabolism are considered to leading to obesity and its related metabolic complications. N-nicotinamide methyltransferase (NNMT) is a methyltransferase, which participate fully in the synthesis of N1-methylnicotinamide MNAM and S-adenosine homocysteine (SAH) catalyzed by universal methyl donor S-adenosine methionine (SAM) [15, 26, 38]. NNMT is highly expressed in adipose tissue and the liver, emerging as a novel and important player in regulating whole-body energy homeostasis, which is partly due to histone methylation and NAD + content increasement [12, 17, 29]. In our previous study, we found that cold exposure can temporarily reduce the lipogenesis in liver and increase the gluconeogenesis by enhancing NAD + /NADH metabolism, which is helpful to maintain the lipid and glucose homeostasis systematically [34].

Recently, Yamaguchi et al. reported that NAD + biosynthesis mediated by nicotinamide phosphoribosyl transferase (Nampt) in adipose tissue is of great importance for the regulation of adaptive thermogenesis, lipolysis, and systemic energy metabolism [37]. However, the dynamic change of NAD + -related enzymes in the different types of adipose tissues under cold exposure is more comprehensive, and its important role in the mitochondrial metabolic balance has not yet been documented. In this study, we planned to investigate the changes regarding NAD-synthesizing and NAD-consuming enzymes and their role in the energy metabolism in different adipose tissues of male C57BL/6 mice exposed to cold environment (from 0 to 5 days, respectively). At the cellular level, we also observed the effects of β3-adrenoceptor agonist (CL316, 243) on the expression of NAD + -related enzymes in primary brown adipocytes (BA) and white adipocytes (WA) from male C57BL/6 mice. In order to identify the relationship between the NAD + /NADH metabolism and beige adipogenesis, we also determined the correlation of NNMT and the browning markers in vivo and in vitro.

Materials and methods

Mouse colonies and cold exposure

All animal protocols were approved by the ethics committee of Xi'an Jiaotong University, China. This study was approved by the animal protection and utilization committee of Xi'an Jiaotong University (no.: xjtu-2012–03-06–0037).

The male mice used in this study were in the C57BL/6 background and were bred and maintained under specific pathogen free (SPF) conditions with a 12-h light/12-h dark cycle. Mice were maintained singe-housed and had ad libitum access to water and regular chow diet. After 1 week of adaptation, they were randomly divided into 6 groups: room temperature (RT) which were maintained between 22 and 23 °C for 5 days and cold exposure ($n = 6$ days for each group) for 1, 2, 3, 4, and 5 days, respectively, the same as our previous study [14]. After animal protocols were completed, mice were anesthetized using isoflurane and subsequently sacrificed. All efforts were made to minimize animal suffering. Next, the interscapular BAT (iBAT), subcutaneous WAT (sWAT), and epididymal WAT (eWAT) [7, 33] were dissected and immediately processed or flash-frozen in liquid nitrogen. Tissue samples were stored at – 80 °C until further use to extract RNA and proteins.

Adipocyte culture

Previously described procedures were used [18, 19]. Briefly, iBAT and sWAT were isolated from 3-week-old C57BL/6 male mice for the culture of primary mice BA and WA. The white preadipocytes and the brown preadipocytes were maintained at 37 °C and 5% CO_2. Post-confluent preadipocytes were cultured in a standard differentiation medium to induce the process differentiation.

CL316, 243 treatment

The cells were fully differentiated after 9 days of culture in the differentiation medium. The cells were treated with 0.5 μM, 1.0 μM, or 2.0 μM CL316, 243 (Tocris Bioscience, Bristol, UK), respectively, for 24 h after the deprivation of fetal bovine serum for 12 h. After CL316, 243 treatment, mature adipocytes were lysed in Trizol for RNA extraction and in cold RIPA for protein extraction.

Gene expression analysis

Trizol (Invitrogen, San Diego, USA) was used to isolate the total RNA of both tissues and cells. The mRNA samples were reverse transcribed into cDNA using a commercial RT-PCR Kit according to the manufacturer's instructions (Thermo Scientific, Waltham, USA). Real-time PCR was performed using a commercial RT-PCR Kit according to the manufacturer's instructions (TaKaRa, Japan) as previously described [14]. Briefly, the relative expression of the gene of interest were normalized to the amount of

cyclophilin mRNA as the housekeeping gene using the –ΔΔCt method. Primers synthesized by AUGCT (Beijing, China) and the sequences are listed in Table 1.

Western blotting analysis

Procedures were used as previously described [17, 18]. Briefly, protein samples (20 μg) were separated using 10% SDS-PAGE gels and then transferred to polyvinylidene difluoride membranes (Millipore, Bedford, MA, USA). Membranes were blocked with 5% nonfat dry milk in TBS containing 0.1% Tween for 1 h at room temperature and then blotted with primary antibodies (anti-NAMPT (1:1000) (sc-166866, Santa Cruz, CA, USA), anti-NNMT (1:1000) (ab45652; ab110304, Abcam, Cambridge, MA, USA), anti-Acetyl Lysine (1:1000) (9441 s, Cell Signaling Technology, Danvers, MA, USA), anti-UCP-1 (1:500) (sc6529, Santa Cruz, CA, USA), anti-PGC-1α (1:1000) (ab54481, Abcam, Cambridge, MA, USA), and anti-β-actin (1:1000) (sc-9104) (Santa Cruz Biotechnology Inc., Santa Cruz, CA, USA)) overnight. After washing, membranes were incubated with a secondary horseradish peroxidase (HRP)-coupled antibody and visualized using Immobilon HRP substrate (Millipore). The density of the bands was quantified using Image Lab software (Bio-Rad). The ratio of the intensity of the target protein to that of β-actin loading control was calculated to represent the expression level of the protein. And the normalization was carried out with reference to the total lane protein as determined using a stain-free technology by Bio-Rad.

*Concentration determination of NAD + *

NAD + levels were determined using LC–MS (liquid chromatography coupled with mass spectrometry) strategy [39]. In brief, 20 mg frozen tissue sample or 100 μg quantified cell protein was thoroughly mixed with 800 μL of cold methanol acetonitrile (v/v, 1:1) via vertexing. And then the mixture was processed with sonication for 1 h in ice baths, and centrifuged at 4 °C for 30 min with a speed of 14,000 g. The supernatants were then harvested and dried under vacuum, 25 μL of 50% acetonitrile solution was added for redissolution, and centrifuged at 4 °C for 30 min with a speed of 16,000 g, and then transferred to the sampling vial for further LC–MS analysis. LC–MS analysis was performed using a Shimadzu Nexera LC-30AD UHPLC system with a Waters® ACQUITY UPLC® BEH Amide column (1.7 μm, 2.1 mm × 100 mm) and an AB SCIEX QTRAP 5500 mass spectrometer. NAD + levels were quantitated based on the peak area compared to a standard curve and normalized to weights of frozen tissues and protein content of adipocytes. A quality control sample was set for a certain number of experimental samples in the sample queue to detect and evaluate the stability and repeatability of the system.

PGC-1α acetylation assays

PGC-1α acetylation was detected by immunoprecipitation [1]. In brief, tissues and cells were lysed in ice-cold lysis buffer containing 50 mM Tris–HCl (pH 8.0), 150 mM NaCl, 0.5% NP-40, 1 mM DTT, and 1 mM PMSF supplemented with a cocktail of protease and phosphatase inhibitors. The lysates were clarified by centrifugation at 12,000 g for 5 min and subjected to immunoprecipitation. Then, 100 μg of protein extract was incubated with an anti-PGC-1α antibody (1:1000) (sc-518025, Santa Cruz, CA, USA) for 3 h at 4 °C, followed by a second incubation of 3 h at 4 °C with protein (A + G) agarose beads (Beyotime Company, Shanghai, China). The beads were washed three times, solubilized in 40 μL of 2 × SDS sample buffer. And then the PGC-1α levels and acetylation were detected using specific antibodies for PGC-1α (1:1000) (ab54481, Abcam, Cambridge, MA, USA) and acetyl lysine (1:1000) (9441 s, Cell Signaling Technology, Danvers, MA, USA), respectively. PGC-1α

Table 1 Primers used for quantitative real-time PCR analysis

acb	Accession No	Forward primer	Reverse primer
Nnmt	NM_010924	TGTGCAGAAAACGAGATCCTC	AGTTCTCCTTTTACAGCACCCA
Nampt	NM_021524	GCAGAAGCCGAGTTCAACATC	TTTTCACGGCATTCAAAGTAGGA
Nmnat1	NM_133435	TGGCTCTTTTAACCCCATCAC	TCTTCTTGTACGCATCACCGA
Nrk1	NM_145497	TCATTGGAATTGGTGGTGTGAC	CAACAGGAAACTGCTGACATCAT
Cyp2e1 Cd38	NM_021282 NM_007646	CGTTGCCTTGCTTGTCTGGA GACGCT GCCTCATCTACACT	AAGAAAGGAATTGGGAAA GGTCC TCTTGGAAACAAATG CTCCT
Ucp-1	NM_009463	CTGCCAGGACAGTACCCAAG	TCAGCTGTTCAAAGCACACA
Pgc-1α	NM_008904	CCCTGCCATTGTTAAGACC	TGCTGCTGTTCCTGTTTTC
Cyclophilin	NM_134084	CATACAGGTCCTGGCATCTTGTC	AGACCACATGCTTGCCATCCAG

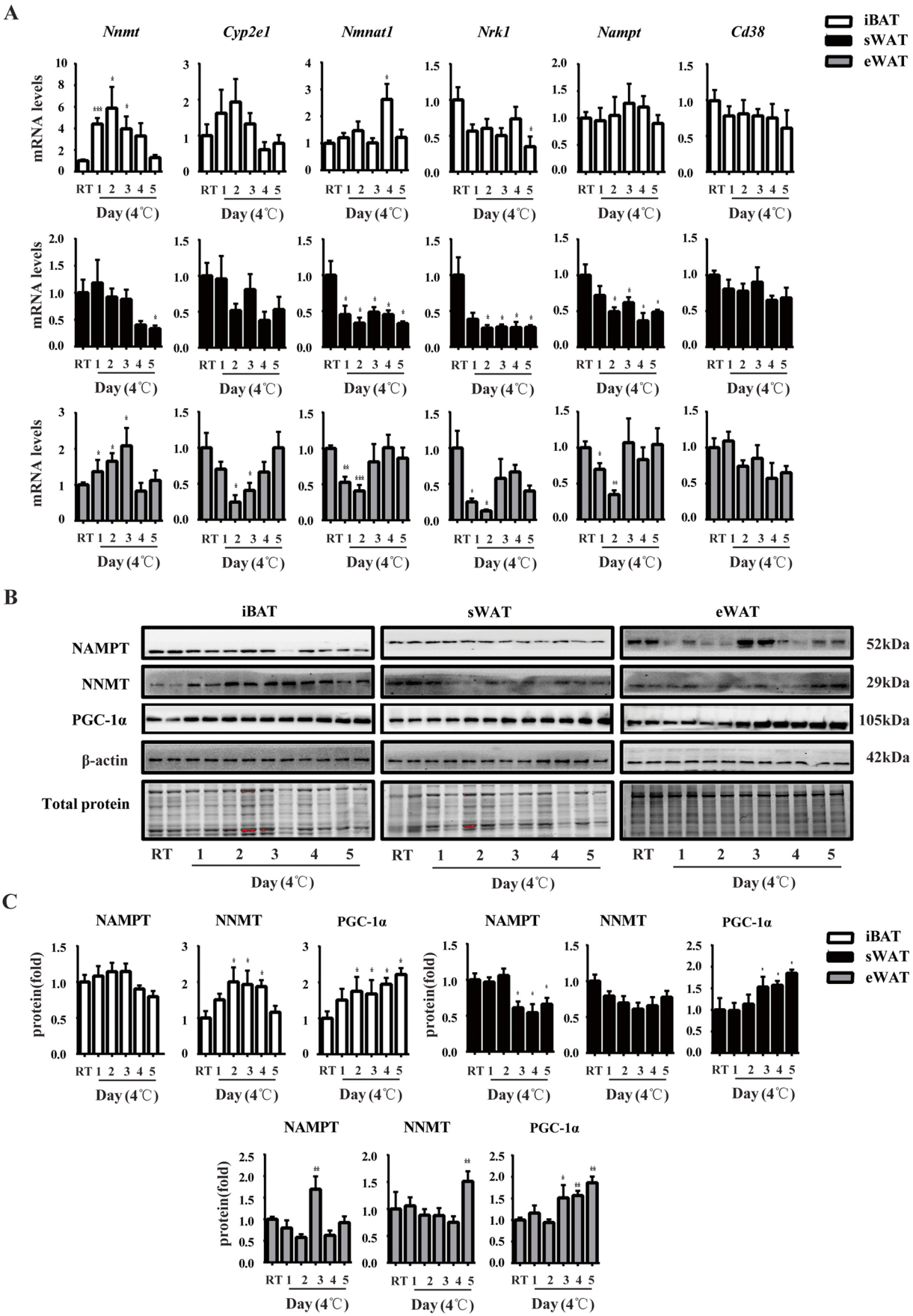
A
Nnmt
Cyp2e1
Nmnat1
Nrk1
Nampt
Cd38
iBAT
sWAT
eWAT
mRNA levels
RT 1 2 3 4 5
Day (4℃)
B
iBAT
sWAT
eWAT
NAMPT
NNMT
PGC-1α
β-actin
Total protein
52kDa
29kDa
105kDa
42kDa
RT 1 2 3 4 5
Day (4℃)
C
NAMPT
NNMT
PGC-1α
protein(fold)
iBAT
sWAT
eWAT
RT 1 2 3 4 5
Day (4℃)

◂**Fig. 1** Dynamic changes in the expression of NAD + metabolism-related enzymes among the adipose tissues during cold exposure. **A** Quantitative PCR analysis of NAD + metabolism-related enzymes genes expression in iBAT, sWAT, and eWAT of control mice and mice exposed to cold (4 °C) up to 5 days. The data show the fold changes of the expressions for the target genes in iBAT, sWAT, and eWAT of RT mice ($n = 6$ for each group). Values are mean ± S.E.M., and expression of genes is corrected for the housekeeping gene *cyclophilin*. (*$P < 0.05$, **$P < 0.01$, ***$P < 0.001$ vs. the expression level of RT group). **B** Western blotting analysis for NAMPT, NNMT, and PGC-1α using total protein isolated from iBAT, sWAT, and eWAT of RT and cold mice ($n = 6$ for each group). **C** Quantification of Western blotting analysis. Protein content is expressed relative to the control and represents three independent experiments with triplicate observations in each experiment. Volume is the sum of all pixel intensities within a band. All data are normalized to the total lane protein and are expressed as mean ± S.E.M. (*$P < 0.05$, **$P < 0.01$, ***$P < 0.001$ vs. the expression level of RT group)

acetylation levels were obtained by acetyl lysine levels normalized to total PGC-1α levels.

Statistical analysis

All statistical analysis was performed with GraphPad Prism 6.0 (GraphPad Software, La Jolla, CA, USA). Data were expressed as means ± S.E.M. of independent experiments. Normality of the data was checked by Shapiro–Wilk test. Comparisons among groups were performed by one-way analysis of variance (one-way ANOVA) in conjunction with Tukey's post hoc test (nonskewed variables) and Kruskal–Wallis test (skewed variables) to compare the differences between the treatment groups. An inverse correlation was defined as $r = -1$ and a direct correlation as $r = +1$ following a Pearson correlation test. Differences were considered statistically significant when $P < 0.05$.

Results

Dynamic changes in the expression of NNMT and its related enzymes among the adipose tissues during cold exposure

In order to clarify the effect of browning on the NAD + metabolism at different time points, we first investigated the expression level of *Nnmt* and related enzymes in the different adipose tissues after the cold exposure. In iBAT, the mRNA level of *Nnmt* increased significantly in the first 3 days and then came to the basal line in the following 2 days of the cold exposure. And the mRNA level of cytochrome P450 2E1 (Cyp2e1), another key gene of NAD + clearance pathway, also showed the same tendency exactly, but without statistical significance. Interestingly, as for other NAD + metabolism-related enzymes, the mRNA level of *Nmnat1* increased significantly at the day 4 and nicotinamide riboside kinase 1(*Nrk1*) decreased significantly at day 5 of the cold exposure, respectively, while the mRNA level of *Nampt*, and the key NAD consuming enzyme, cluster of differentiation 38 (*Cd38*) showed no significant difference during the cold exposure in iBAT (Fig. 1A).

In sWAT, the expression of *Nnmt* was down-regulated and showed the significant difference at day 5 of the cold exposure. The mRNA levels of *Nmnat1*, *Nampt*, and *Nrk1* exhibited a rapid and sustained down-regulation significantly throughout the whole process, while the expression of *Cyp2e1* and *Cd38*, two enzymes related to NAD + clearance pathway, were decreased but showed no significant difference during the cold exposure (Fig. 1A).

In eWAT, cold exposure induced a gradual increase in the expression of *Nnmt* in the first 3 days and then decreased to the basal line in the latter 2 days of the treatment. Notably, the mRNA levels of *Nampt*, *Nmnat1*, *Nrk1*, and *Cyp2e1* were all significantly decreased in the earlier stage and recovered in the next 2 or 3 days. It is somewhat unexpected that the mRNA level of *Cd38* showed an obvious decreasing tendency but no significant change during the cold treatment (Fig. 1A).

To extend our observations at the gene level, we characterized the effects of cold exposure on the changes in the proteins NNMT and NAMPT. Western blotting analysis showed that NNMT and NAMPT protein exhibited a similar expression pattern like their gene expression, respectively, both in iBAT and sWAT. However, perhaps surprisingly, NNMT and NAMPT protein was found to be increased significantly at day 5 and day 3, respectively, in eWAT, while they showed no obvious change in the other time points (Fig. 1B and C). These data demonstrate that cold exposure induces the changes of NNMT mRNA expression in all depots. However, the relative expression of the other markers of NAD and the magnitude of the changes and the temporal profiles differed across the different adipose tissues. Moreover, we found the PGC-1α protein level increased significantly since day 2 and day 3 in iBAT and WAT, respectively (Fig. 1B and C), which was consistent with the gene expression profile of that in our previous study [13].

Dynamic changes in the NAD + metabolism of the different adipose tissues during cold exposure

To demonstrate the role of NAD + metabolism during the beige adipogenesis, we next analyzed how the NAD + levels were affected in different adipose tissues after cold exposure. As shown in Fig. 2A, NAD + concentration in iBAT was not changed in the first 3 days and then increased significantly at day 4 and day 5, while the NAD + concentration were increased significantly at the last 3 days but not changed in the first 2 days of the cold accumulation both in sWAT and eWAT. Since the acetylation status was a post-translational

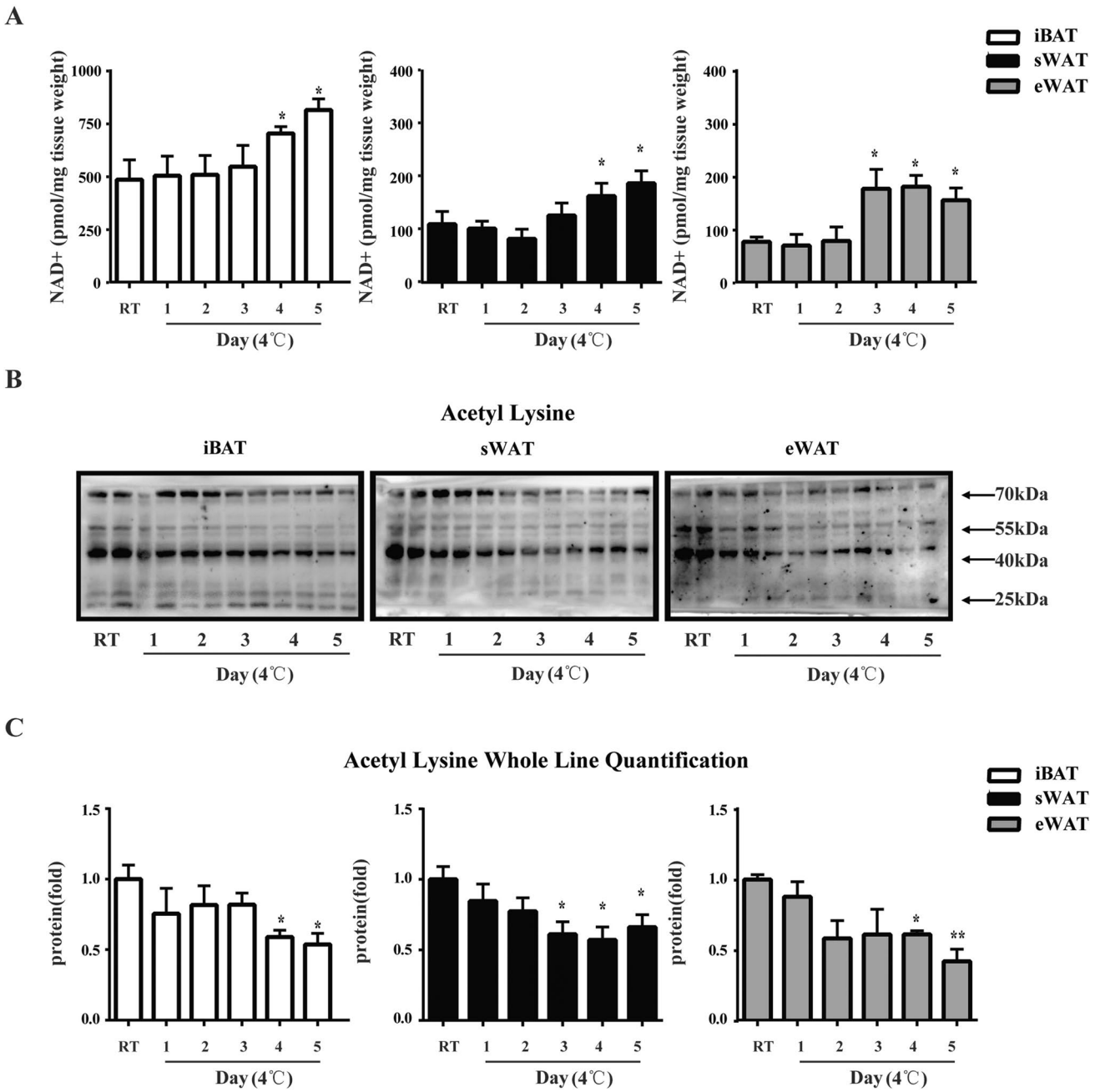

Fig. 2 Cold exposure causes decreased global lysine acetylation among the adipose tissues. **A** Effects of cold exposure on NAD + levels in different adipose tissues. **B** Global lysine acetylation was measured by Western blotting analyses. **C** Lane intensity was quantified and used to determine effects of cold exposure on lysine acetylation. Volume is the sum of all pixel intensities within a band. All data are normalized to the total lane protein and are expressed as mean ± S.E.M. (*$P < 0.05$, **$P < 0.01$ vs. the expression level of RT group)

modification of lysine residues and reflected the NAD + accumulation level in cells, we then analyzed the acetylation status of the adipose tissues using Western blotting analysis. An obvious tendency towards decreased acetylation following cold exposure was observed in all the adipose tissues (Fig. 2B). The difference was that there was not a statistical decrease of the acetylation in iBAT or eWAT until day 4 and day 5, while the decrease came to a statistical difference from day 3 in sWAT (Fig. 2C). This change then persisted throughout the experiment, supporting the results of NAD + quantification changes. Hence, cold exposure not only cause changes to NAD-associated enzymes, but also rapidly affected the lysine acetylation and NAD + level in the adipose tissues in a depot-specific manner.

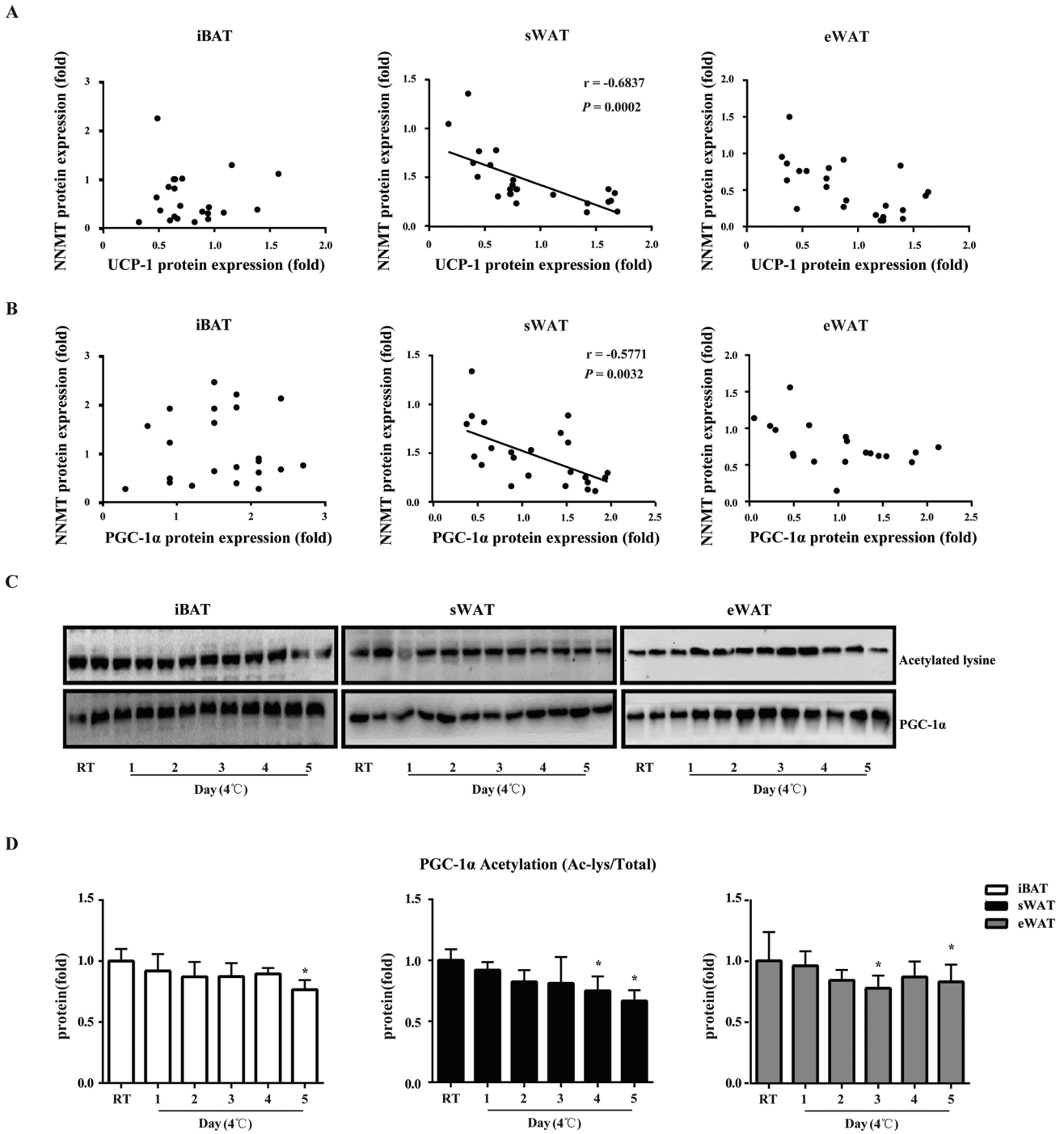

Fig. 3 NNMT expression negatively correlates with browning marker expression at protein level in sWAT but not in iBAT in vivo. Partial regression plots of NNMT protein expression with relative gene expression of browning marker genes **A** UCP-1 protein and **B** PGC-1α protein in iBAT, sWAT, and eWAT at different time of cold treatment, respectively. **C** Western blotting analysis for PGC-1α deacetylation using immunoprecipitation. **D** Quantification of Western blotting analysis for PGC-1α deacetylation. Protein content is expressed relative to the control with triplicate observations in each experiment. Volume is the sum of all pixel intensities within a band. All data are normalized to the total lane protein and are expressed as mean ± S.E.M. ($n = 6$ for each group, $^{*}P < 0.05$, $^{**}P < 0.01$ vs. the expression level of RT group). All experimental mice from six groups (RT and cold mice) were analyzed for correlation ($n = 28$–30)

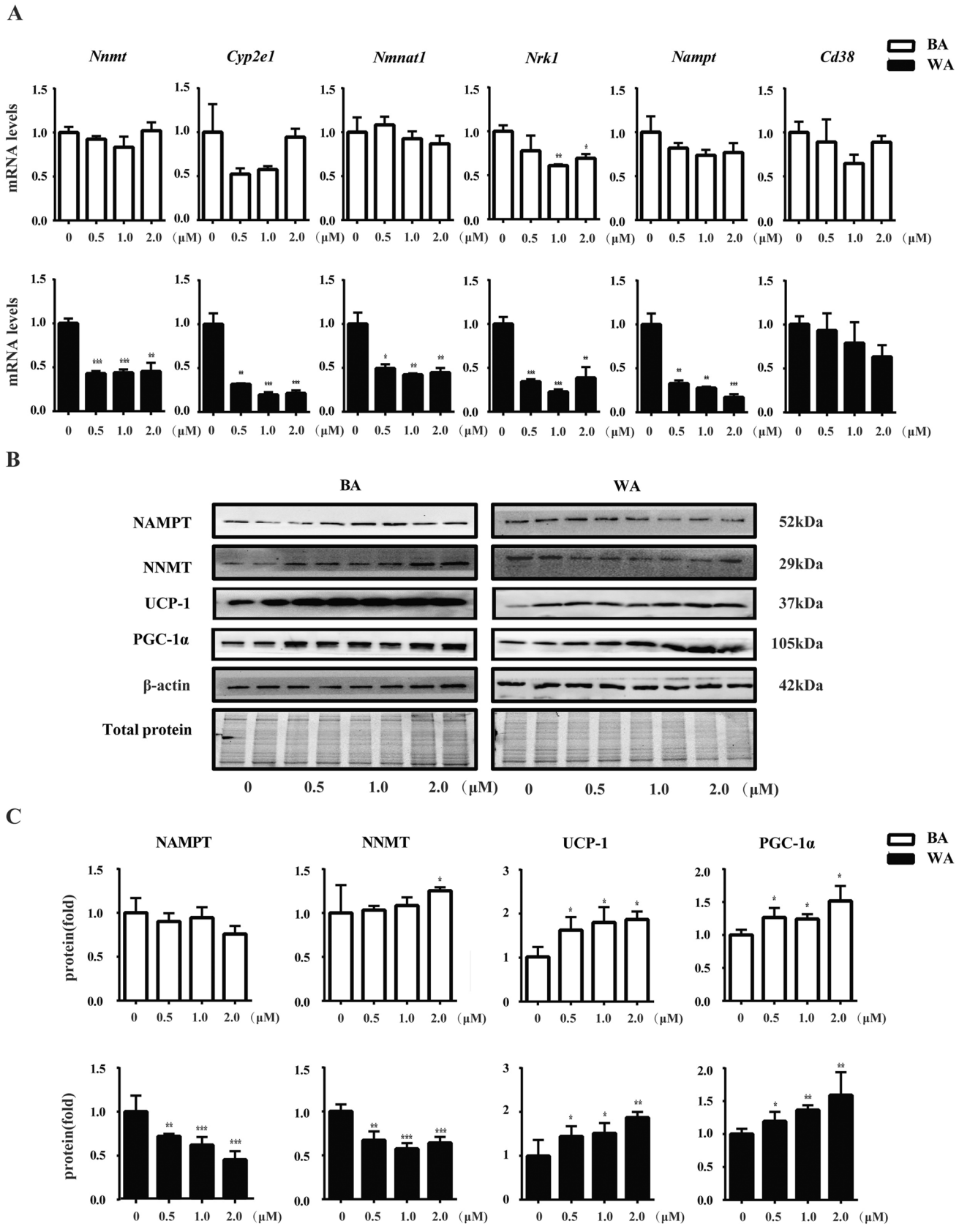
A
Nnmt
Cyp2e1
Nmnat1
Nrk1
Nampt
Cd38
BA
WA
mRNA levels
0 0.5 1.0 2.0 (μM)
B
BA
WA
NAMPT
NNMT
UCP-1
PGC-1α
β-actin
Total protein
52kDa
29kDa
37kDa
105kDa
42kDa
0 0.5 1.0 2.0 (μM)
C
NAMPT
NNMT
UCP-1
PGC-1α
BA
WA
protein(fold)
0 0.5 1.0 2.0 (μM)

◂**Fig. 4** CL316, 243 treatment alters the expressions of NAD + metabolism-related enzymes in BA and WA. **A** Quantitative PCR analysis of NAD + metabolism-related enzymes gene expressions in cultured mice mature BA and WA after different doses of CL316, 243 (0 μM, 0.5 μM, 1.0 μM, and 2.0 μM) treatment up to 24 h. The data show the fold changes of the expression for the target genes in BA and WA at vehicle groups. Values are mean ± S.E.M. from three independent experiments with duplicate wells for each dose of the treatment. The expression of genes is corrected for the housekeeping gene *cyclophilin* (*$P < 0.05$, **$P < 0.01$, ***$P < 0.001$ vs. the expression level of vehicle group). **B** Western blotting analysis for NAMPT, NNMT, UCP-1, and PGC-1α using total protein isolated from BA and WA after different doses of CL316, 243 (0 μM, 0.5 μM, 1.0 μM, and 2.0 μM) treatment up to 24 h ($n = 3$ independent experiments). **C** Quantification of Western blotting analysis. Protein content is expressed relative to the control and represents three independent experiments with triplicate observations in each experiment. Volume is the sum of all pixel intensities within a band. All data are normalized to the total lane protein and are expressed as mean ± S.E.M. (**$P < 0.01$, ***$P < 0.001$ vs. the expression level of vehicle group)

Depot-specific correlations of NNMT protein level with browning markers under cold acclimation in vivo

To explore the potential role of NNMT in the energy metabolism during the beige adipogenesis, we examined the correlations of NNMT protein level with the browning markers UCP-1 and PGC-1α protein expressions in iBAT, sWAT, and eWAT (the protein expression levels of UCP-1 was examined in our previous study [12]). We found significant inverse correlations between NNMT and UCP-1 at protein level in sWAT, but not in iBAT or eWAT (Fig. 3A). As shown in Fig. 3B, there was also a remarkable negative correlation in NNMT and PGC-1α at protein level in sWAT. Interestingly, there was not a significant correlation between NNMT and PGC-1α at protein level in iBAT or eWAT. Moreover, PGC-1α acetylation level decreased significantly at day 5 in iBAT, at day 4 and day 5 in sWAT, and at day 3 and day 5 in eWAT respectively(Fig. 3C A and D). Combined with the fact that cold exposure triggered an acute response of NNMT in iBAT, these observations suggest that the role of NNMT in iBAT may not be regulated by the browning-related mitochondrial activation directly. However, at the same time, the expression of NNMT showed a negative correlation significantly with the browning markers in sWAT. This result indicated that NNMT plays an important role in the energy metabolic homeostasis in sWAT during browning.

Changes in the expression of NNMT and its related enzymes under CL316, 243 treatment in brown adipocyte (BA) and white adipocyte (WA)

In order to verify the effects of different intensity of cold exposure on the changes of NNMT and its related enzymes in different adipose tissues, we conducted the experiment on cultured adipocytes to observe their expression patterns under different doses of CL316, 243 treatment in vitro. In the present study, we provided clear evidences that the NAD + metabolism-related genes including *Nnmt*, *Nampt*, *Nmnat1*, *Cyp2e1*, and *Nrk1* all expressed significantly lower after CL316, 243 treatment in WA without does independent manner. Still to our surprise, the mRNA level of *Cd38* decreased but showed no statistical difference after any dose of CL316, 243 treatment in WA. However, except for *Nrk1*, which is important to maintain NAD homeostasis and maintain tumor cell-line growth upon NAMPT inhibition, expressed significantly lower under 1.0 μM and 2.0 μM CL316, 243 in BA. The mRNA expression levels of other NAD + metabolism-related genes including *Nnmt*, *Nmnat1*, *Nampt*, *Cyp2e1*, and *Cd38* were not observed obvious difference after CL316, 243 treatment in BA (Fig. 4A).

We further investigated the effects of different doses of CL316, 243 on the changes in the proteins NNMT and NAMPT in WA and BA. Unexpectedly, the expression level of NNMT was increased after the 2.0 μM CL316, 243 treatment for 24 h. Moreover, no obvious difference has been observed in the protein of NAMPT in BA among the control and CL316, 243 treatment groups. While similar to their gene expression patterns, the proteins NNMT and NAMPT in WA dropped under 0.5 μM of CL316, 243 and then decreased persistently to a significant lower level at 2.0 μM CL316, 243 treatment (Fig. 4B and C). These expression profiles in WA and BA in response to different doses of CL316, 243 further reinforce the notion that the expression of NNMT and its related enzymes during the browning process exhibits depot-specificity and relates with the process of beige adipogenesis. Moreover, we found the UCP-1 and PGC-1α protein level increased significantly both in BA and WA under any dose of CL316, 243 (Fig. 4B and C), which was consistent with the gene expression profile of that in our previous study [19].

Dynamic changes in the NAD + metabolism under CL316, 243 treatment in BA and WA

We further investigated whether the NAD + levels and acetylation status of BA and WA were changed after different doses of CL316, 243 treatment. It was observed that the NAD + concentration was not increased significantly until 2.0 μM CL316, 243 treatment in BA, while it was increased significantly at any dose of the CL316, 243 treatment in WA (Fig. 5A). What's more, we found that CL316, 243 treatment induced a deacetylation both in BA and WA (Fig. 5B). The lysine acetylation in BA was decreased and showed significant difference under 2.0 μM CL316, 243. In contrast, the lysine acetylation in WA was decreased rapidly and showed significant difference under any dose of CL316, 243 (Fig. 5C). This deacetylation level together with the changes

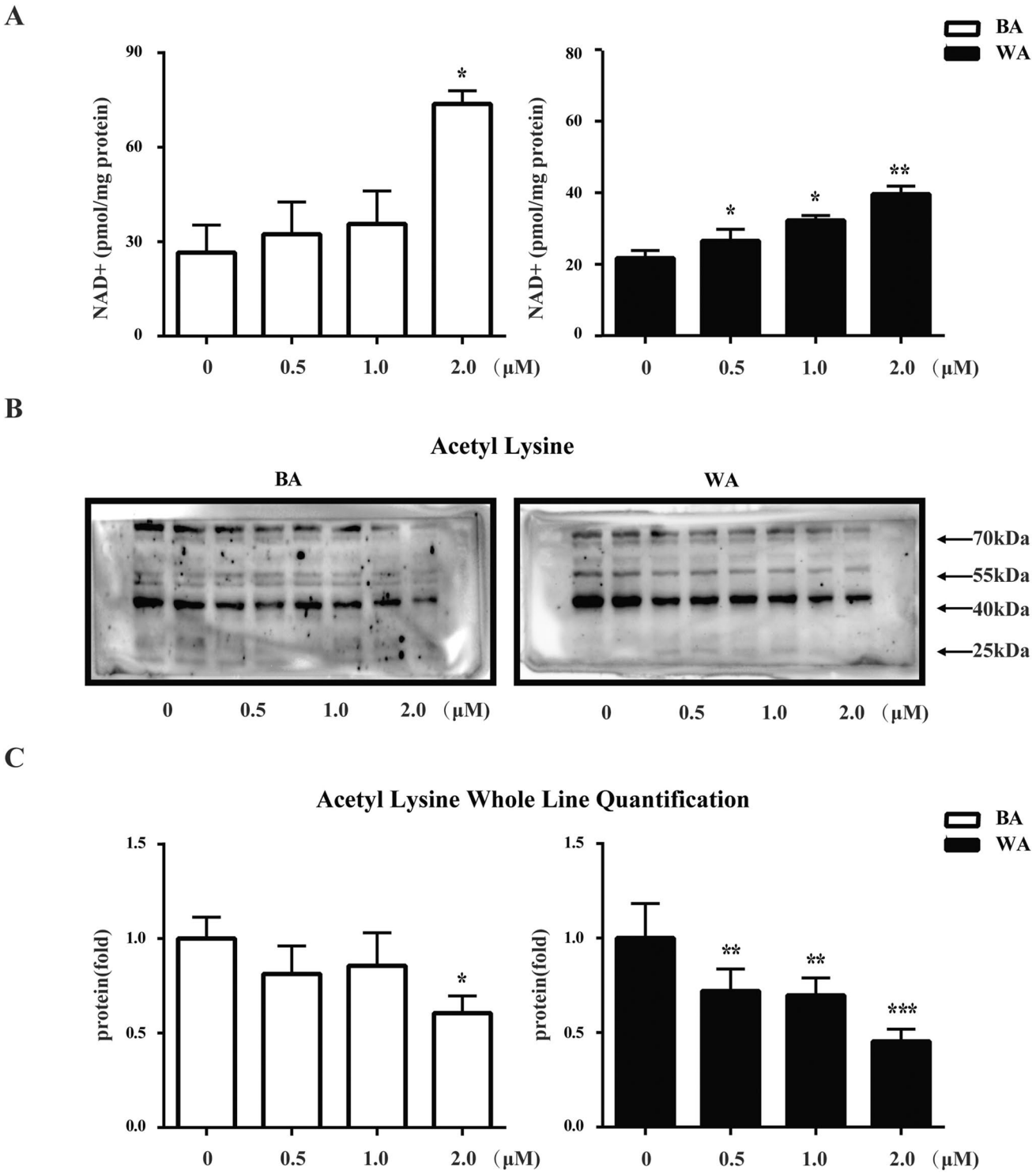

Fig. 5 CL316, 243 causes decreased global lysine acetylation among the adipocytes. **A** The NAD + levels in different adipocytes upon CL316, 243 treatment. **B** Global lysine acetylation was measured by Western blotting analyses in BA and WA ($n = 3$ independent experiments). **C** Lane intensity was quantified and used to determine effects of CL316, 243 on lysine acetylation. Volume is the sum of all pixel intensities within a band. All data are normalized to the total lane protein and are expressed as mean ± S.E.M. (*$P < 0.05$, **$P < 0.01$, ***$P < 0.001$ vs. the expression level of vehicle group)

of the NAD + concentration also exhibited a depot-specific and dynamic manner after CL316, 243 treatment, indicating that the role of NAD + metabolism during the beige adipogenesis is various in different adipocytes.

Depot-specific correlations of NNMT protein level with browning markers under CL316, 243 treatment in vitro

After figuring out the details of the depot-specific expression of NNMT and its related enzymes induced by CL316, 243 treatment in vitro, we investigated the correlations of NNMT protein level with the browning markers UCP-1 and PGC-1α protein expression in WA and BA. As shown in Fig. 6A, it is clear that there was strong negative correlation between NNMT and UCP-1 after CL316, 243 treatment at protein level in WA. In contrast, NNMT level was found to be not correlated with UCP-1 protein expression in BA. As shown in Fig. 6B, there was a significant negative correlation in NNMT and PGC-1α protein level in WA, but not in BA. This result is consistent with the finding of the correlations in vivo, which further suggested that NNMT is a key regulator in the balance of energy metabolism during the browning process in WAT but not BAT. The PGC-1α acetylation level decreased significantly under 2.0 μM of CL316, 243 in BA while decreased in WA under any dose of CL316, 243 (Fig. 6C and D). This result is consistent with the finding of the correlations in vivo, which further suggested that NNMT is a key regulator in the balance of energy metabolism during the browning process in WAT but not BAT.

Discussion

Despite our better understanding of the pathophysiology of obesity, the strategy for obesity treatment is lagging [11]. As we all know, one potential contributing factor for obesity is mitochondrial dysfunction in adipocytes. Mitochondria are central organelles in energy metabolism, and many of the mitochondrial enzymatic pathways rely on the catabolic oxidative reactions, which is dependent on the proper NAD + redox balance [5, 20, 39]. Notably, obesity is associated with disturbed adipose tissue NAD + homeostasis [22, 24].

In recent years, beige adipogenesis is found to increase energy expenditure to overcome energy intake and may lead to a new direction for the treatment of obesity and metabolic syndrome [4]. Although steady progress has been made in mapping the browning of adipose tissues and clarifying the mechanism involved, the field is complex and still in its infancy. In our latest study, we demonstrated that hepatic NAD + /SIRT metabolism was induced during the "cold remodeling" phase and correlated with the decreasing lipogenic and increasing gluconeogenic gene expression, contributing to the maintenance of whole-body lipid and glucose homeostasis [34]. In addition, Yamaguchi et al. demonstrated that NAD + metabolism is essential for the thermogenesis in adipose tissue [37]. A master regulator for mitochondrial function, PGC-1α, coordinately upregulated the enzymes of the de novo NAD biosynthetic pathway from amino acids in a PGC-1α transgenic mouse model [32]. What's more, it was demonstrated that PGC-1α knockout mice developed local deficiency of the NAD precursor niacinamide (NAM), and exogenous NAM improves their local low NAD levels and adipose tissue accumulation [8]. Here we observed that PGC-1α was upregulated and NAD + content was increased during the beige adipogenesis, which was consistent with previous study [2, 37]. What's more, the global lysine acetylation was decreased, which reflect the NAD + accumulation in cells [9, 28, 31]. All these indicated that the preservation of adequate NAD + homeostasis is most likely essential for the browning of adipose tissue and the mitochondrial health of adipocyte.

As a clearance enzyme in the NAD + metabolism pathway, NNMT showed depot-specific response to cold stimulation in adipose tissues in this study. The expression of *Nnmt* mRNA in iBAT and eWAT was increased significantly in the early stage of the cold acclimation, suggesting that cold exposure triggered a significant stress response of NNMT in iBAT and eWAT. The protein expression of NNMT in iBAT and eWAT showed a tendency to rise first and then fall, while it was decreased gradually in sWAT, which might be attribute to the hysteresis of translation and the balance of NNMT among the different adipose tissues.

More recent researches have gradually revealed that excess nicotinamide could induce the toxic effect of metabolic syndrome related by depleting methyl library freedom, influencing NAD-dependent enzymatic reaction, and triggering oxidative stress response [16]. Its toxic effects included impaired glucose tolerance, insulin resistance, elevated liver enzymes, steatosis induced, and fatty liver. Interestingly, we found that gene expression of key enzymes in the NAD + salvage biosynthesis pathway, like NAMPT, NMNAT1, and NRK1, were all decreased during the first 2 days of cold exposure in eWAT. Another nicotinamide clearance enzyme, Cyp2e1, was decreased from day 2 to day 3. The weakened NAD + salvage pathway and nicotinamide clearance pathway may lead to the accumulation of nicotinamide in eWAT. Thus, our present findings indicated that NNMT was triggered to clean the extra nicotinamide in the "cold remodeling" phase to protect the toxic effects and fell to the resting state in the "cold adapted" phase in eWAT. After that, the expression of key enzymes in the NAD + salvage biosynthesis pathway picked up and also the declined of *Nnmt* expression leading to the increased NAD + level at the "cold remodeling" phase in eWAT. Besides, Rudolphi

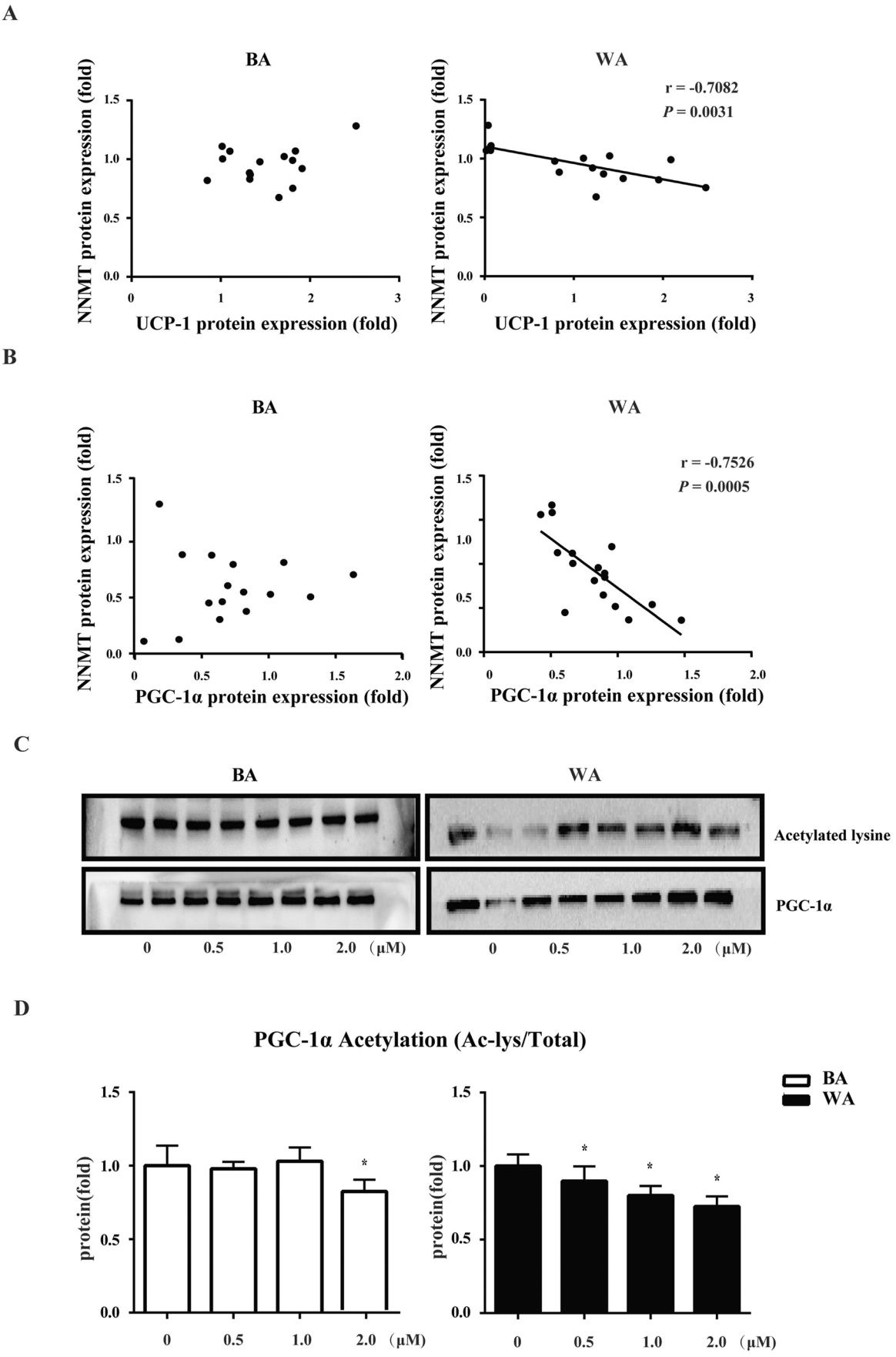
A
BA
WA
r = -0.7082
P = 0.0031
NNMT protein expression (fold)
UCP-1 protein expression (fold)
B
BA
WA
r = -0.7526
P = 0.0005
NNMT protein expression (fold)
PGC-1α protein expression (fold)
C
BA
WA
Acetylated lysine
PGC-1α
0 0.5 1.0 2.0 (μM)
D
PGC-1α Acetylation (Ac-lys/Total)
BA
WA
protein(fold)
0 0.5 1.0 2.0 (μM)

◂**Fig. 6** NNMT protein expression negatively correlates with browning marker expression in WA but not in BA in vitro. Partial regression plots of NNMT protein expression with relative expression of browning marker genes **A** Ucp-1 protein and **B** PGC-1α protein in BA and WA under different doses of CL316, 243 treatment, respectively. **C** Western blotting analysis for PGC-1α deacetylation using Immunoprecipitation. **D** Quantification of Western blotting analysis for PGC-1α deacetylation. Protein content is expressed relative to the control and represents three independent experiments with triplicate observations in each experiment. Volume is the sum of all pixel intensities within a band. All data are normalized to the total lane protein and are expressed as mean ± S.E.M. (*$P < 0.05$, **$P < 0.01$, ***$P < 0.001$ vs. the expression level of vehicle group). All experimental adipocytes from four groups (vehicle and CL316, 243 groups) were analyzed for correlation ($n = 15$–16)

et al. showed that body weight predicts NNMT activity in eWAT, but not in sWAT or iBAT, as obesity develops [25]. Combined with the expression pattern of *Nnmt* in eWAT after cold treatment and the increased NAD + level during the cold exposure, it indicated the important role of NNMT in eWAT during the cold-induced browning of adipose tissues.

Moreover, the mRNA levels of enzymes involved in the NAD + salvage synthesis pathway, including *Nmnat1*, *Nampt*, and *Nrk1* exhibited a rapid and sustained down-regulation throughout the whole process in sWAT, which can be attributed to the inflammation and oxidative stress and support the previous research findings [30]. Nevertheless, the expression patterns of *Nmnat1*, *Nampt*, *Nrk1*, and *Cyp2e1* were decreased significantly in the first 2 or 3 days and then climbed up back after. It was suggested the increased NAD + level might depend on the other synthetases or the de novo NAD + synthesis pathway, and this need to be considered in future studies.

For more than a decade, the lipolytic hydrolysis of triglycerides in BAT has been considered essential for cold-induced non-shivering thermogenesis [3]. While a bit of a surprise, there was no significant change in the expression of rate-limiting NAD biosynthesis enzymes, NAMPT and NMNAT1, in iBAT during the "cold remodeling" phase (day 1 to day 3) in this study. Consistently, Yamaguchi et al. recently showed that the brown adipocyte-specific *Nampt* knockout mice had normal thermogenic and lipolytic responses [37]. In addition, we performed the correlation analyses and found negative correlations between the protein expressions of NNMT and the browning markers UCP-1and PGC-1α in sWAT and WA, but not in iBAT or BA. We speculate that more NAM enters into NAD + synthesis through the salvage pathway to generate more NAD + in response to upregulation of UCP1 and PGC-1α upon cold stimulation. As a result, less NAM needs to be methylated by NNMT, and negative correlation with thermogenesis markers was observed in the sWAT. All these suggested that iBAT might not be the target organ of the regulation of NAD-related lipolysis metabolism during the adipose tissue browning. This discovery is also supported by the study of Schreiber et al., which demonstrated that adipose triglyceride lipase-mediated lipolysis in BAT is not a prerequisite for cold-induced non-shivering thermogenesis in vivo [27]. Furthermore, Bruce Spiegelman et al. and other groups have identified the additional mechanisms for activating thermogenesis beyond UCP-1[6, 13], while recent studies have demonstrated that the adrenergic stimulation of BA would result in acute fission of the mitochondrial network which is also implicated in thermogenesis [34, 35]. These alternative pathways for the generation of heat beyond BAT and UCP-1 might also explain our findings about the NAD + metabolism in iBAT after cold exposure.

Our studies also reveal that, similar to the expression pattern of all the NAD + metabolism-related genes in sWAT, their mRNA levels decreased significantly after CL316, 243 treatment in WA. Moreover, the expression of NNMT showed strong negative correlations with both UCP-1 and PGC-1α in WA, which were similar to the results of that in vivo, suggesting that Nnmt is a robust regulated gene in response to energy balance challenge during beige adipogenesis. These results essentially accorded with our finding of time course of the beige adipogenesis [13], which suggested that NAD + metabolism may exert a depot-specific effect on the energy metabolism among the adipose tissues.

However, Yamaguchi et al. found that NAMPT levels in BAT were increased [37], while Benzi et al. found that CD38 levels were decreased significantly in BAT and WAT after cold exposure [2]. In contrast, we did not find these changes in our animals during cold exposure. An explanation for these conflicting data should be the difference in housing temperature, as well as the different time lengths of cold exposure.

Conclusion

Based on the current finding demonstrated here, we are closer to understanding the complex mechanism behind browning-associated regulation of NNMT. In conclusion, the browning process alters the NNMT expression in adipose tissues with depot specificity dynamically. In sWAT, the expression of NNMT decreased significantly and showed negative correlation with browning markers during the cold treatment. In eWAT, this key enzyme in NAD + clearance pathway was stimulated after 2 and 3 days of cold exposure and then returned to control levels by day 4. This key time coincided exactly with a "cold remodeling" phase (days 1–3) of the cold-induced transformation process [14]. While in iBAT, NNMT expression increased first then declined to basal line but exhibited no correlation with UCP-1 and PGC-1α after the cold exposure. To sum up, NNMT in WAT is more responsive to cold exposure than in BAT, and

NNMT may contribute to the process of beige adipogenesis in a depot-specific manner.

Acknowledgements We gratefully thank the Shanghai Bioprofile Biotechnology Co., Ltd. (Shanghai, China) for technological assistance in targeted metabolomics experiment.

Author contribution Conceptualization, R.J. and X.W.; methodology, R.J.; validation, R.J., X.W. and X.L.; formal analysis, J.J.; investigation, Z.Y.; resources, J.H.; data curation, J.L.; writing, original draft preparation, R.J.; writing, review and editing, X.W.; visualization, R.J.; supervision, J.Y.; project administration, X.L.; funding acquisition, X.W., J.Y and X.L.. All authors have read and agreed to the published version of the manuscript.

Funding This work was supported by the National Natural Science Foundation of China (No. 81871190 and 81700773); and the Natural Science Foundation of Shaanxi Province, China (No. 2020JQ-565 and 2017JM3023); and the Fundamental Research Funds for the Central Universities (xzy012019106).

Data availability All raw data that support the findings of this study will be available without restriction from the corresponding author on reasonable request.

Declarations

Ethics approval This research was involved animal protocols, and all animal protocols were approved by the ethics committee and the animal protection and utilization committee of Xi'an Jiaotong University, China (no.: xjtu-2012–03-06–0037).

Consent to participate Not applicable.

Conflict of interest The authors declare no competing interests.

References

1. Amorim JA, Sinclair DA (2021) Measuring PGC-1alpha and its acetylation status in mouse primary myotubes. Methods Mol Biol 2310:301–309. https://doi.org/10.1007/978-1-0716-1433-4_17
2. Benzi A, Sturla L, Heine M, Fischer AW, Spinelli S, Magnone M, Sociali G, Parodi A, Fenoglio D, Emionite L, Koch-Nolte F, Mittrucker HW, Guse AH, De Flora A, Zocchi E, Heeren J, Bruzzone S (2021) CD38 downregulation modulates NAD(+) and NADP(H) levels in thermogenic adipose tissues. Biochim Biophys Acta Mol Cell Biol Lipids 1866:158819. https://doi.org/10.1016/j.bbalip.2020.158819
3. Cannon B, Nedergaard J (2004) Brown adipose tissue: function and physiological significance. Physiol Rev 84:277–359. https://doi.org/10.1152/physrev.00015.2003
4. Cao L, Choi EY, Liu X, Martin A, Wang C, Xu X, During MJ (2011) White to brown fat phenotypic switch induced by genetic and environmental activation of a hypothalamic-adipocyte axis. Cell Metab 14:324–338. https://doi.org/10.1016/j.cmet.2011.06.020
5. Caton PW, Kieswich J, Yaqoob MM, Holness MJ, Sugden MC (2011) Nicotinamide mononucleotide protects against pro-inflammatory cytokine-mediated impairment of mouse islet function. Diabetologia 54:3083–3092. https://doi.org/10.1007/s00125-011-2288-0
6. Chouchani ET, Kazak L, Spiegelman BM (2019) New advances in adaptive thermogenesis: UCP1 and beyond. Cell Metab 29:27–37. https://doi.org/10.1016/j.cmet.2018.11.002
7. Cinti S (2005) The adipose organ. Prostaglandins Leukot Essent Fatty Acids 73:9–15. https://doi.org/10.1016/j.plefa.2005.04.010
8. Collier JB, Whitaker RM, Eblen ST, Schnellmann RG (2016) Rapid renal regulation of peroxisome proliferator-activated receptor gamma coactivator-1alpha by extracellular signal-regulated kinase 1/2 in physiological and pathological conditions. J Biol Chem 291:26850–26859. https://doi.org/10.1074/jbc.M116.754762
9. Etchegaray JP, Mostoslavsky R (2016) Interplay between metabolism and epigenetics: a nuclear adaptation to environmental changes. Mol Cell 62:695–711. https://doi.org/10.1016/j.molcel.2016.05.029
10. Gesta S, Tseng YH, Kahn CR (2007) Developmental origin of fat: tracking obesity to its source. Cell 131:242–256. https://doi.org/10.1016/j.cell.2007.10.004
11. Hill JO, Wyatt HR, Peters JC (2012) Energy balance and obesity. Circulation 126:126–132. https://doi.org/10.1161/CIRCULATIONAHA.111.087213
12. Hong S, Moreno-Navarrete JM, Wei X, Kikukawa Y, Tzameli I, Prasad D, Lee Y, Asara JM, Fernandez-Real JM, Maratos-Flier E, Pissios P (2015) Nicotinamide N-methyltransferase regulates hepatic nutrient metabolism through Sirt1 protein stabilization. Nat Med 21:887–894. https://doi.org/10.1038/nm.3882
13. Ikeda K, Kang Q, Yoneshiro T, Camporez JP, Maki H, Homma M, Shinoda K, Chen Y, Lu X, Maretich P, Tajima K, Ajuwon KM, Soga T, Kajimura S (2017) UCP1-independent signaling involving SERCA2b-mediated calcium cycling regulates beige fat thermogenesis and systemic glucose homeostasis. Nat Med 23:1454–1465. https://doi.org/10.1038/nm.4429
14. Jia R, Luo XQ, Wang G, Lin CX, Qiao H, Wang N, Yao T, Barclay JL, Whitehead JP, Luo X, Yan JQ (2016) Characterization of cold-induced remodelling reveals depot-specific differences across and within brown and white adipose tissues in mice. Acta Physiol (Oxf) 217:311–324. https://doi.org/10.1111/apha.12688
15. Kang-Lee YA, McKee RW, Wright SM, Swendseid ME, Jenden DJ, Jope RS (1983) Metabolic effects of nicotinamide administration in rats. J Nutr 113:215–221. https://doi.org/10.1093/jn/113.2.215
16. Knip M, Douek IF, Moore WP, Gillmor HA, McLean AE, Bingley PJ, Gale EA, European nicotinamide diabetes intervention trial G, (2000) safety of high-dose nicotinamide: a review. Diabetologia 43:1337–1345. https://doi.org/10.1007/s001250051536
17. Kraus D, Yang Q, Kong D, Banks AS, Zhang L, Rodgers JT, Pirinen E, Pulinilkunnil TC, Gong F, Wang YC, Cen Y, Sauve AA, Asara JM, Peroni OD, Monia BP, Bhanot S, Alhonen L, Puigserver P, Kahn BB (2014) Nicotinamide N-methyltransferase knockdown protects against diet-induced obesity. Nature 508:258–262. https://doi.org/10.1038/nature13198
18. Luo X, Jia R, Luo XQ, Wang G, Zhang QL, Qiao H, Wang N, Yan JQ (2017) Cold exposure differentially stimulates angiogenesis in BAT and WAT of mice: implication in adrenergic activation. Cell Physiol Biochem 42:974–986. https://doi.org/10.1159/000478680
19. Luo X, Jia R, Zhang Q, Sun B, Yan J (2016) Cold-induced browning dynamically alters the expression profiles of inflammatory adipokines with tissue specificity in mice. Int J Mol Sci 17https://doi.org/10.3390/ijms17050795
20. Mercader J, Granados N, Caimari A, Oliver P, Bonet ML, Palou A (2008) Retinol-binding protein 4 and nicotinamide phosphoribosyltransferase/visfatin in rat obesity models. Horm Metab Res 40:467–472. https://doi.org/10.1055/s-2008-1065324

21. Nedergaard J, Bengtsson T, Cannon B (2007) Unexpected evidence for active brown adipose tissue in adult humans. Am J Physiol Endocrinol Metab 293:E444-452. https://doi.org/10.1152/ajpendo.00691.2006
22. Pagano C, Pilon C, Olivieri M, Mason P, Fabris R, Serra R, Milan G, Rossato M, Federspil G, Vettor R (2006) Reduced plasma visfatin/pre-B cell colony-enhancing factor in obesity is not related to insulin resistance in humans. J Clin Endocrinol Metab 91:3165–3170. https://doi.org/10.1210/jc.2006-0361
23. Park H, He A, Tan M, Johnson JM, Dean JM, Pietka TA, Chen Y, Zhang X, Hsu FF, Razani B, Funai K, Lodhi IJ (2019) Peroxisome-derived lipids regulate adipose thermogenesis by mediating cold-induced mitochondrial fission. J Clin Invest 129:694–711. https://doi.org/10.1172/JCI120606
24. Rappou E, Jukarainen S, Rinnankoski-Tuikka R, Kaye S, Heinonen S, Hakkarainen A, Lundbom J, Lundbom N, Saunavaara V, Rissanen A, Virtanen KA, Pirinen E, Pietilainen KH (2016) Weight loss is associated with increased NAD(+)/SIRT1 expression but reduced PARP activity in white adipose tissue. J Clin Endocrinol Metab 101:1263–1273. https://doi.org/10.1210/jc.2015-3054
25. Rudolphi B, Zapp B, Kraus NA, Ehebauer F, Kraus BJ, Kraus D (2018) Body weight predicts nicotinamide N-Methyltransferase activity in mouse fat. Endocr Res 43:55–63. https://doi.org/10.1080/07435800.2017.1381972
26. Scheller T, Orgacka H, Szumlanski CL, Weinshilboum RM (1996) Mouse liver nicotinamide N-methyltransferase pharmacogenetics: biochemical properties and variation in activity among inbred strains. Pharmacogenetics 6:43–53. https://doi.org/10.1097/00008571-199602000-00003
27. Schreiber R, Diwoky C, Schoiswohl G, Feiler U, Wongsiriroj N, Abdellatif M, Kolb D, Hoeks J, Kershaw EE, Sedej S, Schrauwen P, Haemmerle G, Zechner R (2017) Cold-induced thermogenesis depends on ATGL-mediated lipolysis in cardiac muscle, but not brown adipose tissue. Cell Metab 26(753–763):e757. https://doi.org/10.1016/j.cmet.2017.09.004
28. Shimazu T, Hirschey MD, Newman J, He W, Shirakawa K, Le Moan N, Grueter CA, Lim H, Saunders LR, Stevens RD, Newgard CB, Farese RV Jr, de Cabo R, Ulrich S, Akassoglou K, Verdin E (2013) Suppression of oxidative stress by beta-hydroxybutyrate, an endogenous histone deacetylase inhibitor. Science 339:211–214. https://doi.org/10.1126/science.1227166
29. Song Q, Chen Y, Wang J, Hao L, Huang C, Griffiths A, Sun Z, Zhou Z, Song Z (2020) ER stress-induced upregulation of NNMT contributes to alcohol-related fatty liver development. J Hepatol 73:783–793. https://doi.org/10.1016/j.jhep.2020.04.038
30. Srivastava S (2016) Emerging therapeutic roles for NAD(+) metabolism in mitochondrial and age-related disorders. Clin Transl Med 5:25. https://doi.org/10.1186/s40169-016-0104-7
31. Su X, Wellen KE, Rabinowitz JD (2016) Metabolic control of methylation and acetylation. Curr Opin Chem Biol 30:52–60. https://doi.org/10.1016/j.cbpa.2015.10.030
32. Tran MT, Zsengeller ZK, Berg AH, Khankin EV, Bhasin MK, Kim W, Clish CB, Stillman IE, Karumanchi SA, Rhee EP, Parikh SM (2016) PGC1alpha drives NAD biosynthesis linking oxidative metabolism to renal protection. Nature 531:528–532. https://doi.org/10.1038/nature17184
33. Walden TB, Hansen IR, Timmons JA, Cannon B, Nedergaard J (2012) Recruited vs. nonrecruited molecular signatures of brown, "brite", and white adipose tissues. Am J Physiol Endocrinol Metab 302:E19-31. https://doi.org/10.1152/ajpendo.00249.2011
34. Wei X, Jia R, Yang Z, Jiang J, Huang J, Yan J, Luo X (2020) NAD(+) /sirtuin metabolism is enhanced in response to cold-induced changes in lipid metabolism in mouse liver. FEBS Lett 594:1711–1725. https://doi.org/10.1002/1873-3468.13779
35. Wikstrom JD, Mahdaviani K, Liesa M, Sereda SB, Si Y, Las G, Twig G, Petrovic N, Zingaretti C, Graham A, Cinti S, Corkey BE, Cannon B, Nedergaard J, Shirihai OS (2014) Hormone-induced mitochondrial fission is utilized by brown adipocytes as an amplification pathway for energy expenditure. EMBO J 33:418–436. https://doi.org/10.1002/embj.201385014
36. Xue B, Coulter A, Rim JS, Koza RA, Kozak LP (2005) Transcriptional synergy and the regulation of Ucp1 during brown adipocyte induction in white fat depots. Mol Cell Biol 25:8311–8322. https://doi.org/10.1128/MCB.25.18.8311-8322.2005
37. Yamaguchi S, Franczyk MP, Chondronikola M, Qi N, Gunawardana SC, Stromsdorfer KL, Porter LC, Wozniak DF, Sasaki Y, Rensing N, Wong M, Piston DW, Klein S, Yoshino J (2019) Adipose tissue NAD(+) biosynthesis is required for regulating adaptive thermogenesis and whole-body energy homeostasis in mice. P Natl Acad Sci USA 116:23822–23828. https://doi.org/10.1073/pnas.1909917116
38. Yan L, Otterness DM, Craddock TL, Weinshilboum RM (1997) Mouse liver nicotinamide N-methyltransferase: cDNA cloning, expression, and nucleotide sequence polymorphisms. Biochem Pharmacol 54:1139–1149. https://doi.org/10.1016/s0006-2952(97)00325-0
39. Yoshino J, Mills KF, Yoon MJ, Imai S (2011) Nicotinamide mononucleotide, a key NAD(+) intermediate, treats the pathophysiology of diet- and age-induced diabetes in mice. Cell Metab 14:528–536. https://doi.org/10.1016/j.cmet.2011.08.014